www.czasopisma.pan.pl PAN www.journals.pan.pl
Chemical and Process Engineering 2018, 39 (2), 223–232
DOI: 10.24425/122945

MATHEMATICAL MODELLING OF GAS FLOW AND DETERMINATION OF AXIAL GAS DISPERSION COEFFICIENTS USING NUMERICAL INVERSE LAPLACE TRANSFORM AND MAPLE® IN A TYPICAL COMMERCIAL APPARATUS

Małgorzata Wójcik*, Mirosław Szukiewicz

Rzeszow University of Technology, Faculty of Chemistry, Department of Chemical and Process Engineering, al. Powstancow Warszawy 6, 35-959 Rzeszow

In this paper, a new simple method for determination of flow parameters, axial dispersion coefficients D_L and Péclet numbers Pe was presented. This method is based on an accurate measurement model considering pulse tracer response. Our method makes it possible to test the character of gas flow motion and precisely measure flow parameters for different pressures and temperatures. The idea of combining the transfer function, numerical inversion of the Laplace transform and optimisation method gives many benefits like a simple and effective way of finding solution of inverse problem and model coefficients. The calculated values of flow parameters (D_L and/or Pe) suggest that in the considered case the gas flow is neither plug flow nor perfect mixing under operation condition. The obtained outcomes agree with the gas flow theory. Calculations were performed using the CAS program type, Maple®.

Keywords: numerical inversion of the Laplace transform, mathematical modelling, axial gas dispersion coefficient, Maple®

1. INTRODUCTION

The Laplace transform is a very powerful analysis tool for the solution of differential and integral equations. However, application of this technique to practical problems is limited, because an analytical inversion of problems to the time domain can be difficult or even impossible to obtain, so numerical methods have to be used. The term *numerical inversion of the Laplace transform* was introduced in the 1960s by Bellman et al. (1967), approximating the Laplace integral by a Gauss–Legendre polynomial. Many algorithms for the numerical computation of the inverse Laplace transform can be found in the literature. There are four main groups: i) the Fourier series method, which is based on the Poisson summation formula, (ii) the Gaver–Stehfest algorithm, which is based on combination of Gaver functionals, (iii) the Weeks method, which is based on bilinear transformations and Laguerre function expansion, (iv) the Talbot method, which is based on deforming the contour in the Bromwich inversion integral (Abate and Valko, 2004), that differ from each other with respect to accuracy, computational time and method parameter choice, which results in their differing scope of applicability. A comprehensive review of methods of the numerical inversion of the Laplace transform based on a comparison of fourteen algorithms in terms of numerical accuracy, computational efficiency and simplicity of implementation is presented by Davies and Martin (1979). Other reviews were given by Duffy (1993), Narayanan and Beskos (1982), and Cohen (2007).

* Corresponding author, e-mail: wojcik.mm@op.plpl, ichms@prz.edu.pl

According to the literature reports, many scientists have recommended numerical algorithms of inverse Laplace transform to find a solution in the time domain of a specific type of problem. *The Gaver–Stehfest method* is a popular numerical inversion method used in groundwater flow and petroleum engineering applications (Yang et al., 2011). This algorithm has been applied successfully by several authors to solving various problems in chemistry (Montella, 2008), geophysics (Knight and Raiche, 1982), mathematics (Endah and Surjanto, 2017), electrical engineering (Smith and Brančik, 2016). *The Gaver–Stehfest method* is often used in engineering fields to solve linear and non-linear diffusion problems. *The Stehfest*, *the Honig and Hirdes*, and *Zakian's methods* were recommended for the dispersion-dominated problems, but for radial dispersion problems – *the de Hoog, the Talbot*, and *the Simon methods* (Wang and Zhan, 2015) are more effective than others. Li-Wei Chiang (1989) presented many methods to obtain a solution of groundwater problems, *the Schapery*, *the Widder*, *the Koizumi*, *the Weeks*, and *the Talbot methods*. Escobar et al. (2014) presented a comparison of two algorithms, *the Stehfest's* and *Iseger's method* to solve two well-known oil-industry reservoir models in the Laplace domain. *The Dubner and Abate method* has been applied to modelling of tracer transport in heterogeneous media, oil and geothermal reservoirs, and in groundwater aquifers (Kocabas, 2011). Chen et al. (1996) employed *the Crump algorithm* to obtain a solution of the radial dispersion in the real-time domain from the Laplace domain. *The de Hoog algorithm* was used to determine the fate and transport of groundwater contaminants (i.e. chromium), biotracers and microorganisms (Boupha et al., 2004). Taiwo et al. (1995) compared and used two methods, *the Honig and Hirdes*, and *Zakian's method* to four typical chemical engineering problems. Also, *Zakian's algorithm* was applied to determine the kinetic parameters for the adsorption of human serum albumin (Taiwo and King, 2003). The application of *the Hosono method* to the determination of the signal velocity in dispersive pulse propagation is presented in (Wyns et al., 1989). *The method of Juraj and Lumboir* was employed to solve an unsteady thin film flow problem of a second grade fluid through a porous medium and estimate fluid parameters (Ali and Awais, 2014).

This article presents a new simple method to determine quantities that characterise gas flow motion (axial dispersion coefficient or a Péclet number). The method is based on a precise measurement instrument model development. The model takes into account the internal construction of an instrument. It was split into separate zones, which differ one from another by geometry, function, or both. A conception of transfer function was applied to simplify analysis and solution of the resultant model. The transfer function is a complex function, known from process control, but this work indicates that it is applicable also out of this field. It is derived using the Laplace transform and, as a result, the application of the numerical inverse Laplace transform method seems to be a logical way of finding solution of the model. In combination with any optimisation method it creates a simple and effective inverse problem solving method. The presented scheme is very advantageous to determine model coefficients and competitive when compared to other methods. The well-known advantages of the transfer function also appear, in particular ease of rebuilding the model, when one part of instrument (e.g. vessel) is exchangeable.

1.1. The Gaver–Stehfest method

The Gaver–Stehfest method is a simple algorithm for the numerical inversion of the Laplace transform, which approximates the time domain solution by the following formula (Zhang, 2007):

$$f(t) = \frac{\ln 2}{t} \sum_{k=1}^{N} V_k F\left(k \frac{\ln 2}{t}\right) \tag{1}$$

$$V_k = (-1)^{k+\frac{N}{2}} \sum_{j=\left(\frac{k+1}{2}\right)}^{\min\left(k,\frac{N}{2}\right)} \frac{j^{\frac{N}{2}}(2j)!}{\left(\frac{N}{2}-j\right)!\,j!\,(j-1)!\,(k-j)!\,(2j-k)!} \tag{1a}$$

where: $F(s) \stackrel{\wedge}{=} f(t)$.

The parameter N is called the Stehfest number N. It is the number of terms used in Eq. (1). Parameter N must be an even integer. The precision of calculation depends on the parameter N because the inversion is based on a summation of N weighted values. Theoretically, a large value of parameter N determines the more accurate solution but if N is too large the results may be worsened due to the round-off errors. In practice, N should be chosen by trial and error method to get the best results. Thus, a suitable choice of the value N is important to achieve the most accurate solution (Hassanzadeh and Pooladi-Darvish, 2007). Many authors propose a different value of the parameter $N$to obtain the most accurate solution. For example, Cheng and Sidauruk (1994) recommended that the optimal choice of N should be within the range from 6 to 20. Our preliminary numerical tests confirmed efficiency of this algorithm for gas flow problems (Wójcik et al., 2015; Wójcik et al., 2017) and on the basis of results performed, $N = 30$ was accepted.

2. DESCRIPTION OF THE EXPERIMENTS

The system was flushed for 15–30 minutes with a constant flow of helium (carrier gas) until a stable TCD signal was received. At the same time, the volume of sample loop (2.50×10^{-7}; 5.000×10^{-7} m^3) was flushed also with a constant flow of nitrogen (tracer). Next, the 8-way valve was opened to allow the flow of helium with the constant volumetric flow rate (of 3.333×10^{-7} or 5.000×10^{-7} or 6.667×10^{-7} m^3/s) at STP through the sample loop, the zones (*vessel* and pipes), and the detector TCD. After all, the TCD signal was recorded.

The experiments have been conducted in New Chemical Synthesis Institute in Puławy (Poland) at each combination of process variable:

- pressure: 1.200×10^5; 2.000×10^5; 3.000×10^5 Pa
- temperature: 313.15; 333.15; 353.15 K.

3. HYDRODYNAMIC MODEL OF GAS FLOW INSIDE APPARATUS

The simplified scheme of measuring system for experiments is shown in Fig. 1. The system consists of the following elements:

1) a unit called *vessel*, consisting of two steel pipes (1a) and (1b). The part of larger diameter (1a) is usually filled with porous pellets (not in experiment described below),
2) the 8-way valve,
3) the sample loop,
4) pipes,
5) the thermal conductivity detector (TCD).

In order to create a mathematical model of the gas flow, the unit between the 8-way valve (1) and the TCD detector (2) was divided into three zones. They are distinguishable on the basis of geometry and/or its function. A volume of the fragment between the 8-way valve and *vessel* is negligible. Geometry of the apparatus was determined on the basis of its technical data and previously made investigations. Table 1 gives a complete list of technical data.

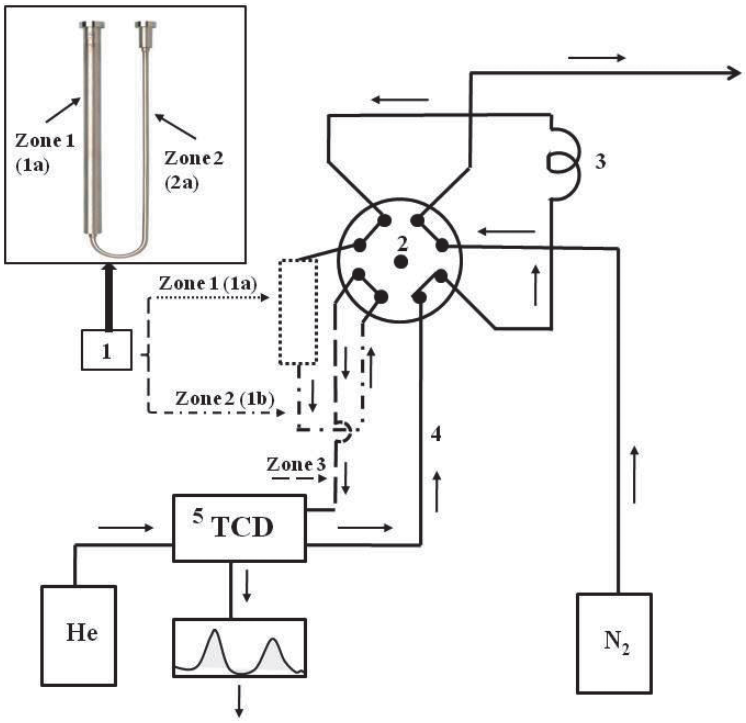

Fig. 1. Simplified schematic representation of apparatus (Micromeritics' AutoChem 2950HP)

Table 1. Technical data

Number of the zone	Description		L_i [m]	$d_{w,i}$ [m]
1	Vessel	1a	1.7700×10^{-1}	7.6500×10^{-3}
2		1b	2.3500×10^{-1}	1.5875×10^{-3}
3	pipe connecting 8-way valve and TCD detector		5.7000×10^{-1}	1.5875×10^{-3}

4. MATHEMATICAL MODEL EMPLOYED IN THIS STUDY

The model is based on the following assumptions:

- the system is operated under isothermal conditions;
- gases satisfy equation of state of an ideal gas.

The mass balance of the tracer (nitrogen) in each zone can be described by the following of partial differential equations and the initial and boundary conditions (Table 2): $c(L_1+L_2+L_3,t)$ corresponds to the concentration recorded by the TCD-detector. In this work, we used a rectangular signal pulse which is given by

$$c_0 = \begin{cases} 0 & t < 0 \\ c_T & 0 \le t \le \dfrac{V_{\text{imp}}}{F_v} \\ 0 & t > \dfrac{V_{\text{imp}}}{F_v} \end{cases} \tag{2}$$

where

$$c_T = \frac{P}{R_g \cdot T}$$

Table 2. Mathematical model

Equation	$\frac{\partial c(x,t)}{\partial t} = D_{L,i}\frac{\partial^2 c(x,t)}{\partial x^2} - \frac{4F_v}{\pi d_{w,i}^2}\cdot\frac{\partial c(x,t)}{\partial x}$		
i-th zone	1	2	3
IC	$c(x,0)=0$	$c(x,0)=0$	$c(x,0)=0$
BC1	*Danckwerts boundary conditions* were used for the closed-closed boundaries as: $\frac{4F_v}{\pi d_{w,i}^2}c_0 = = \frac{4F_v}{\pi d_{w,i}^2}c(0^+,t) - D_{L,i}\frac{\partial c(x,t)}{\partial x}\Big\vert_{x=0^+}$	$c(L_1^+,t) = (L_1^- t)$	$c(L_1+L_2^+,t) = c(L_1+L_2^-,t)$
BC2	$\frac{\partial c(x,t)}{\partial x}\Big\vert_{x=L_i^-} = 0$	$\frac{\partial c(x,t)}{\partial x}\Big\vert_{x=(L_1+L_2)^+} = 0$	$\frac{\partial c(x,t)}{\partial x}\Big\vert_{x=(L_1+L_2+L_3)^+} = 0$

5. RESULTS AND DISCUSSION

To obtain the outlet concentration of tracer, $c(L_1+L_2+L_3,t)$, the following procedure was applied for each zone separately:

- the governing equation with the appropriate initial and boundary conditions was transformed into Laplace domain; as a result the problem is reduced to ordinary differential equation
- the analytic solution of ordinary differential equation was found and, next, an outlet concentration was determined
- the quotient $G_i(s)$ of outlet and inlet concentration was found.

Multiplication of $G_i(s)$ gives:

$$G_1(s)\,G_2(s)\,G_3(s) = \frac{\overline{c}(L_1,s)}{\overline{c}_0(s)}\,\frac{\overline{c}(L_1+L_2,s)}{\overline{c}(L_1,s)}\,\frac{\overline{c}(L_1+L_2+L_3,s)}{\overline{c}(L_1+L_2,s)} = \frac{\overline{c}(L_1+L_2+L_3,s)}{\overline{c}_0(s)} \tag{3}$$

which can be easily rearranged into

$$\overline{c}(L_1+L_2+L_3,s) = G_1(s)\,G_2(s)\,G_3(s)\,\overline{c}_0(s) \tag{4}$$

where

$$G_1(s) = \frac{\overline{c}(L_1,s)}{c_0} = -\frac{8F_v e^{(a+b)L_1}(\pi^2 d_{w,1}^4 D_{L,1}s + F_v^2 - 2F_v c)}{(2F_v-c)(D_{L,1}\pi^2 d_{w,1}^4 s)e^{(a-b)L_1} + 8F_v^2 e^{(a-b)L_1} - 4F_v(e^{(a-b)L_1})c} \tag{4a}$$

$$G_2(s) = \frac{\overline{c}(L_1+L_2,s)}{\overline{c}(L_1,s)} = -\frac{2e^{(d+f)(L_1+L_2)}g}{2F_v e^{(d-f)(L_1+L_2)}e^{(f-d)L_1} - g(e^{(d-f)(L_1+L_2)}e^{(f-d)L_1})} \tag{4b}$$

$$G_3(s) = \frac{\overline{c}(L_1+L_2+L_3,s)}{\overline{c}(L_1+L_2,s)} = -\frac{2e^{(h+i)(L_1+L_2+L_3)}j}{2F_v e^{(h-i)(L_1+L_2+L_3)}e^{(i-h)(L_1+L_2)} - j(e^{(h-i)(L_1+L_2+L_3)}e^{(i-h)(L_1+L_2)})} \tag{4c}$$

where

$$a = \frac{2F_v - \sqrt{D_{L,1}\pi^2 d_{w,1}^4 s + 4F_v^2}}{D_{L,1}\pi d_{w,1}^2}$$

$$b = \frac{2F_v + \sqrt{D_{L,1}\pi^2 d_{w,1}^4 s + 4F_v^2}}{D_{L,1}\pi d_{w,1}^2}$$

$$c = \sqrt{D_{L,1}\pi^2 d_{w,1}^4 s + 4F_v^2}$$

$$d = \frac{2F_v - \sqrt{D_{L,2}\pi^2 d_{w,2}^4 s + 4F_v^2}}{D_{L,2}\pi d_{w,2}^2}$$

$$f = \frac{2F_v + \sqrt{D_{L,2}\pi^2 d_{w,2}^4 s + 4F_v^2}}{D_{L,2}\pi d_{w,2}^2}$$

$$g = \sqrt{D_{L,2}\pi^2 d_{w,2}^4 s + 4F_v^2}$$

$$h = \frac{2F_v - \sqrt{D_{L,3}\pi^2 d_{w,3}^4 s + 4F_v^2}}{D_{L,3}\pi d_{w,3}^2}$$

$$i = \frac{2F_v + \sqrt{D_{L,3}\pi^2 d_{w,3}^4 s + 4F_v^2}}{D_{L,3}\pi d_{w,3}^2}$$

$$j = \sqrt{D_{L,3}\pi^2 d_{w,3}^4 s + 4F_v^2}$$

The complex function $\bar{c}(L_1+L_2+L_3,s)$ was transformed into the real domain applying the Gaver–Stehfest algorithm. $\bar{c}(L_1+L_2+L_3,s)$ corresponds to the function F in Eq. (1).

The values of model parameters $D_{L,i}$ were determined using *trial and error procedure* (determining preliminary values) and inner optimisation procedure *NLP Solve* of the program Maple® (improving precision). As the correct value of parameter $D_{L,i}$ was accepted the one with the lowest value of the standard deviation between the numerical and experimental results (solution of the inverse problem). All calculations were carried out with precision up to 64 decimal digits using Maple®17.

The Péclet number is defined by

$$Pe = \frac{vL_i}{D_{L,i}} \tag{5}$$

Results are shown in Tables 3 and 4. We assumed that $D_{L,2} = D_{L,3}$ due the same diameter of pipes (see Tables 3 and 4).

As can be seen from Table 3, the values of the axial dispersion coefficient increase with temperature and decrease with increasing pressure. These observations agree with the flow theory.

The calculated values of Péclet numbers (see Table 4) indicate that gas flow is neither ideal plug flow nor perfect mixing in the tested system.

www.czasopisma.pan.pl PAN www.journals.pan.pl

Table 3. Values of axial dispersion coefficients

P [Pa]	V_{imp} [m^3]						Number of zone	F_v [m^3/s]
	2.500×10^{-7}			5.000×10^{-7}				
	T [K]							
	313.15	333.15	353.15	313.15	333.15	353.15		
	D_L [m^2/s]							
1.200×10^5	7.937×10^{-5}	8.403×10^{-5}	9.236×10^{-5}	7.705×10^{-5}	8.456×10^{-5}	9.348×10^{-5}	1	3.333×10^{-7}
	2.753×10^{-3}	3.525×10^{-3}	3.625×10^{-3}	2.472×10^{-3}	2.705×10^{-3}	2.799×10^{-3}	2, 3	
	7.597×10^{-5}	8.157×10^{-5}	8.776×10^{-5}	7.516×10^{-5}	8.085×10^{-5}	9.017×10^{-5}	1	5.000×10^{-7}
	4.757×10^{-3}	5.217×10^{-3}	5.289×10^{-3}	4.363×10^{-3}	4.918×10^{-3}	4.989×10^{-3}	2, 3	
	7.480×10^{-5}	8.092×10^{-5}	8.844×10^{-5}	7.579×10^{-5}	8.179×10^{-5}	9.009×10^{-5}	1	6.667×10^{-7}
	7.502×10^{-3}	8.073×10^{-3}	8.549×10^{-3}	7.299×10^{-3}	8.069×10^{-3}	7.406×10^{-3}	2, 3	
2.000×10^5	4.919×10^{-5}	5.235×10^{-5}	5.679×10^{-5}	4.879×10^{-5}	5.275×10^{-5}	5.620×10^{-5}	1	3.333×10^{-7}
	1.437×10^{-3}	1.399×10^{-3}	1.375×10^{-3}	9.419×10^{-4}	8.459×10^{-4}	7.273×10^{-4}	2, 3	
	4.846×10^{-5}	5.173×10^{-5}	5.573×10^{-5}	4.825×10^{-5}	5.232×10^{-5}	5.559×10^{-5}	1	5.000×10^{-7}
	1.873×10^{-3}	2.088×10^{-3}	2.147×10^{-3}	1.019×10^{-3}	9.724×10^{-4}	1.007×10^{-3}	2, 3	
	4.795×10^{-5}	5.118×10^{-5}	5.502×10^{-5}	4.849×10^{-5}	5.200×10^{-5}	5.547×10^{-5}	1	6.667×10^{-7}
	3.095×10^{-3}	3.325×10^{-3}	3.460×10^{-3}	1.755×10^{-3}	1.893×10^{-3}	1.967×10^{-3}	2, 3	
3.000×10^5	3.329×10^{-5}	3.474×10^{-5}	3.747×10^{-5}	3.412×10^{-5}	3.586×10^{-5}	3.716×10^{-5}	1	3.333×10^{-7}
	1.041×10^{-3}	1.258×10^{-3}	1.255×10^{-3}	6.909×10^{-4}	7.338×10^{-4}	7.803×10^{-4}	2, 3	
	3.253×10^{-5}	3.483×10^{-5}	3.752×10^{-5}	3.346×10^{-5}	3.530×10^{-5}	3.717×10^{-5}	1	5.000×10^{-7}
	1.619×10^{-3}	1.569×10^{-3}	1.609×10^{-3}	1.271×10^{-3}	1.257×10^{-3}	1.195×10^{-3}	2, 3	
	3.262×10^{-5}	3.511×10^{-5}	3.747×10^{-5}	3.372×10^{-5}	3.570×10^{-5}	3.774×10^{-5}	1	6.667×10^{-7}
	2.289×10^{-3}	2.172×10^{-3}	2.171×10^{-3}	1.541×10^{-3}	1.389×10^{-3}	1.216×10^{-3}	2, 3	

Table 4. Values of Péclet numbers

P [Pa]	V_{imp} [m^3]						Number of zone	F_v[m^3/s]
	2.500×10^{-7}			5.000×10^{-7}				
	T [K]							
	313.15	333.15	353.15	313.15	333.15	353.15		
	Pe [–]							
1.200×10^5	18	18	17	19	18	17	1	3.333×10^{-7}
	14	11	12	15	15	15	2	
	42	35	36	47	46	47	3	
	28	28	27	28	28	27	1	5.000×10^{-7}
	12	12	12	13	12	13	2	
	37	35	37	40	35	39	3	
	38	37	36	38	37	36	1	6.667×10^{-7}
	10	10	10	10	10	12	2	
	31	31	31	32	31	35	3	
2.000×10^5	17	17	17	18	17	17	1	3.333×10^{-7}
	16	17	19	24	29	35	2	
	48	53	36	74	88	108	3	
	26	26	26	27	26	26	1	5.000×10^{-7}
	18	17	18	33	47	38	2	
	56	53	55	102	146	117	3	
	36	36	35	35	35	35	1	6.667×10^{-7}
	15	15	15	26	26	26	2	
	45	45	45	79	78	80	3	
3.000×10^5	17	17	17	17	17	17	1	3.333×10^{-7}
	15	13	14	22	22	22	2	
	45	39	42	67	67	67	3	
	26	26	26	26	26	26	1	5.000×10^{-7}
	14	15	16	18	19	21	2	
	43	47	49	55	59	66	3	
	35	35	34	34	34	34	1	6.667×10^{-7}
	13	15	16	20	23	28	2	
	41	45	48	60	71	86	3	

6. CONCLUSIONS

The main results of this paper can be summarised as follows:

- Application of the Gaver–Stehfest algorithm is suitable for solution of the model of gas flow. It works fast and with high accuracy. An additional advantage is its simplicity.
- The value of axial dispersion coefficient can easily be determined.
- The gas flow is neither plug flow nor perfect mixing under operation condition.

- The Computer Algebra System (CAS) – Maple® is very helpful for researchers to transform model equations to the Laplace domain, solve the resultant set of equations and execute the inverse Laplace transform properly and without errors.
- The pulse tracer technique, the Laplace transform and modern software system simplify analysis of the task and make it possible to determine gas dispersion coefficients without any problems.

SYMBOLS

$c(L_1+L_2+L_3,t)$	outlet concentration of tracer, mol/m^3
$\bar{c}(L_i,s)$	solution of model for zone in Laplace domain, $i=1\ldots3$
$\bar{c}_0$	inlet concentration of tracer, mol/m^3
$D_{L,i}$	axial dispersion coefficient in *i-th* zone, m^2/s, $i=1\ldots3$
$d_{w,i}$	diameter of the zone, m, $i=1\ldots3$
F_v	volumetric flow rate, m^3/s
$G_i(s)$	transfer function for zone, $i=1\ldots3$
L_i	length of *i-th* zone, m, $i=1\ldots3$
N	number of terms used in numerical approximation
P	pressure, Pa
Pe	Péclet number
R_g	universal gas constant, J $\cdot$ mol$^{-1}\cdot$K^{-1}
s	Laplace transform parameter
T	temperature, K
V_{imp}	volume of sample loop, m^3
v	gas flow velocity, m/s

The authors would like to thank Researches from New Chemical Synthesis Institute in Pulawy (Poland) for sharing the experimental data.

REFERENCES

Abate J., Valko P., 2004. Multi-precision Laplace transform inversion. *Int. J. Numer. Meth. Engng.*, 60, 979–993. DOI: 10.1002/nme.995.

Ali M., Awais M., 2014. Laplace transform method for unsteady thin film flow of a second grade fluid through a porous medium. *J. Mod. Phys.*, 5, 103–106. DOI: 10.4236/jmp.2014.53017.

Bellman R.E., Kalaba R.E., Lockett J., 1967. Numerical inversion of Laplace transforms. *IEEE Trans. Autom. Control*, 12, 624–625. DOI: 10.1109/TAC.1967.1098700.

Boupha K., Jacobs J.M., Hatfield K., 2004. MDL Groundwater software: Laplace transforms and the De Hoog algorithm to solve contaminant transport equation. *Comput. Geosci.*, 30, 445–453. DOI: 10.1016/j.cageo.2004.02.001.

Cheng A.H-D., Sidauruk P., 1994. Approximate inversion of the Laplace transform. *Mathematica Journal*, 4(1), 76–82.

Chen J.S., Liu C.W., Chenb C.S., Yehc H.D., 1996. A Laplace transform solution for tracer tests in a radially convergent flow field with upstream dispersion. *J. Hydrol.*, 183, 263–275. DOI: 10.1016/0022-1694(95)02972-9.

Chiang L.-W., 1989. *The application of numerical Laplace inversion methods to groundwater flow and solute transport problems*. New Mexico Institute of Mining and Technology, New Mexico.

Cohen A.M., 2007. *Numerical methods for Laplace transform inversion*. Springer, Boston, MA. DOI: 10.1007/978-0-387-68855-8.

Davies B., Martin B., 1979. Review Numerical Inversion of the Laplace transform: A survey and comparison of methods. *J. Comput. Phys.*, 33, 1–32. DOI: 10.1016/0021-9991(79)90025-1.

Duffy D.G., 1993. On the numerical inversion of Laplace transform: comparison of three new methods on characteristic problems from applications. *ACM Trans. Math. Software*, 19, 333–359. DOI: 10.1145/155743.155788.

Endah R.M., Surjanto S. D., 2017. Performance of Gaver-Stehfest numerical Laplace inversion method on option pricing formulas. *Int. J. Comput. Sci. Appl. Math.*, 3, 71–76. DOI: 10.12962/j24775401.v3i2.2215.

Escobar F.H., Leguizamo F.A., Cantillo J.H., 2014. Comparison of Stehfest's and Iseger's algorithms for Laplacian inversion in pressure well tests. *J. Eng. Appl. Sci.*, 9(6), 919–922.

Hassanzadeh H., Pooladi-Darvish M., 2007. Comparison of different numerical Laplace inversion methods for engineering applications. *Appl. Math. Comput.*, 189, 1966–1981. DOI: 10.1016/j.amc.2006.12.072.

Knight J.H., Raiche A.P., 1982. Transient electromagnetic calculations using the Gaver- Stehfest inverse Laplace transform method. *Geophys.*, 47, 47–50. DOI: 10.1190/1.1441280.

Kocabas I., 2011. Application of iterated Laplace transformation to tracer transients in heterogeneous porous media. *J. Franklin Inst.*, 348, 1339–1362. DOI: 10.1016/j.jfranklin.2010.04.002.

Montella C., 2008. LSV modelling of electrochemical systems through numerical inversion of Laplace transforms, I: The GSLSV algorithm. *J. Electroanal. Chem.*, 614, 121–130. DOI: 10.1016/j.jelechem.2007.11.010.

Narayanan G.V., Beskos D.E., 1982. Numerical operational methods for time-dependent linear problems. *Int. J. Numer. Methods Eng.*, 18, 1829–1854. DOI: 10.1002/nme.1620181207.

Smith N., Brancik L., 2016. Comparative study on one-dimensional numerical inverse Laplace transform methods for electrical engineering. *Elektrorevue*, 18(1), 1–6.

Taiwo O., King R., 2003. Determination of kinetic parameters for the adsorption of a protein on porous beads using symbolic computation and numerical Laplace inversion. *Chem. Eng. Process.*, 42, 561–568. DOI: 10.1016/S0255-270(02)00068-5.

Taiwo O., Schultz J., Krebs V., 1995. A comparison of two methods for the numerical inversion of Laplace transforms. *Comp. Chem. Eng.*, 19, 303–308. DOI: 10.1016/0098-1354(94)00055-S.

Wang Q., Zhan H., 2015. On different numerical inverse Laplace methods for solute transport problems. *Adv. Water Resour.*, 75, 80–92. DOI: 10.1016/j.advwaters.2014.11.001.

Wójcik M., Szukiewicz M., Kowalik P., 2015. Application of numerical Laplace inversion methods in chemical engineering with Maple® . *J. Appl. Comp. Sci. Methods*, 7, 5–15. DOI: 10.1515/jacsm-2015-0006.

Wójcik M., Szukiewicz M., Kowalik P., Próchniak W., 2017. The efficiency of the Gaver-Stehfest method to solve one-dimensional gas flow model. *Adv. Sci Technol. Res. J.*, 11(1), 246–252. DOI: 10.12913/22998624/68138.

Wyns P., Foty D.P., Oughstun K.E., 1989. Numerical analysis of the precursor fields in linear dispersive pulse propagation. *J. Opt. Soc. Am. A*, 6, 1421–1429. DOI: 10.1364/JOSAA.6.001421.

Yang F., Wang X., Liu H., 2011. Application of Laplace transform in well test interpretation – an example of Tahe oil field cavity – fractured reservoirs in Tarim Basin. *2011 International Conference on Multimedia Technology (ICTM)*, IEEE, Hangzhou, China, 26–29 July 2011, 1988–1991. DOI: 10.1109/ICMT.2011.6002378.

Zhang J., 2007. Some innovative numerical approaches for pricing American options. *University of Wollongong Thesis Collection*, Wollongong, Australia.

Received 16 September 2017
Received in revised form 03 May 2018
Accepted 17 May 2018